effect, which was previously known only in electrochemical systems involving modified electrodes, may now be applied to polyelectrolyte-stabilized colloidal systems. This effect will result in inhibition, though not prevention, of the catalytic pathway when the number of charges on the radical is smaller. However, under conditions where the radical concentration is extremely low, the competing disproportionation process is prevented and a redox reaction can be obtained. Therefore, in the design of efficient photocatalytic systems, one should limit the use of polyelectrolyte stabilizers for colloidal catalysts in systems involving oppositely charged radicals. Such systems should be avoided altogether if the radical bears multiple charges, with the exception of conditions where the radicals are extremely stable.

Acknowledgment. I am indebted to Dr. P. Neta for his advice and encouragement in carrying out this work, to Dr. R. E. Sassoon for critically reviewing this manuscript, and to the National Institute of Standards and Technology for hosting me as a guest scientist. This research was supported by the Office of Basic Energy Research of the U.S. Department of Energy under Contract No. DE-AI05-83ER13108 with NIST.

Registry No. PSS, 50851-57-5; $ZnTMPyP^{5+}$, 79346-64-8; $ZnTMPyP^{4+}$, 40603-58-5; IrO_x, 12645-46-4; $IrCl_6^{3-}$, 14648-50-1; $Ir(OH)_6^{2-}$, 61703-90-0; NaN_3, 26628-22-8.

Reaction of Acetaldehyde and Acetyl Radical with Atomic and Molecular Oxygen

Akira Miyoshi, Hiroyuki Matsui,

Department of Reaction Chemistry, Faculty of Engineering, The University of Tokyo, 7-3-1, Hongo, Bunkyo-ku, Tokyo 113, Japan

and Nobuaki Washida*

Division of Atmospheric Environment, The National Institute for Environmental Studies, P.O. Tsukuba-gakuen, Ibaraki 305, Japan *(Received: December 20, 1988; In Final Form: March 7, 1989)*

The reaction of acetaldehyde with atomic oxygen, $O(^3P)$, was studied by the discharge-flow–photoionization mass spectrometry method at room temperature (295 ± 4 K) for the conditions of excess atomic oxygen. The rate constant for reaction 1, $CH_3CHO + O \rightarrow CH_3CO + OH$, was (3.9 ± 0.3) × 10^{-13} cm^3 $molecule^{-1}$ s^{-1}. Branching fractions for the subsequent reactions 2a, $CH_3CO + O \rightarrow CH_2CO + OH$, and 2b, $CH_3CO + O \rightarrow CH_3 + CO_2$, were determined to be 22 ± 5% and 76 ± 24%, respectively. The experiments in the presence of molecular oxygen show that the ratio of rate constants for reaction 3, $CH_3CO + O_2 + M \rightarrow CH_3CO_3 + M$, to reaction 2 is (6.3 ± 0.5) × 10^{-3} [total pressure 3.6 Torr (He)]. From the rate constant for reaction 3 obtained by McDade et al., the rate constant for reaction 2 was calculated: k_2 = (3.2 ± 0.7) × 10^{-10} cm^3 $molecule^{-1}$ s^{-1}. When the concentration of molecular oxygen increased, the yields of both CH_3 and CH_2CO decreased. From this decrease, the branching fractions for reactions 4a, $CH_3CO_3 + O \rightarrow CH_2CO + OH + O_2$, and 4b, $CH_3CO_3 + O \rightarrow CH_3 + CO_2 + O_2$, were determined: <10% and 27 ± 25%, respectively. A discussion of the other products from $CH_3CO_3 + O$ is presented.

Introduction

Acetaldehyde and acetyl radical are important chemical species in combustion and atmospheric chemistry. In low-temperature combustion such as cool flames and hydrocarbon oxidations in the induction period, aldehydes, acyl radicals, and acylperoxy radicals play important roles.[1] In the atmosphere, acetyl radicals are formed in the reactions of acetaldehyde with OH,[2] Br,[3] and Cl.[4] Also, they are believed to be the source of acetylperoxy radicals, which lead to PAN (peroxyacetyl nitrate).

The reaction of acetaldehyde with atomic oxygen has been studied by Mack and Thrush,[5] Singleton et al.,[6] and Michael and Lee.[7]

$$CH_3CHO + O(^3P) \rightarrow CH_3CO + OH \qquad (1)$$

These studies measured the decay of oxygen atoms and thus needed stoichiometric corrections,[5] or very low atomic oxygen concentrations (or radical scavengers), to avoid the influence of subsequent reactions. Reaction 1 proceeds via abstraction of the weakly bonded aldehydic hydrogen and yields CH_3CO.[8] Then, the dominant subsequent reaction in the presence of excess atomic oxygen is

$$CH_3CO + O \rightarrow \begin{cases} CH_2CO + OH & (2a) \\ CH_3 + CO_2 & (2b) \end{cases}$$

Reaction 2 should have two pathways, 2a and 2b, by analogy with O + alkyl radical reactions[9,10] and the O + HCO reaction.[11] In these systems, products are observed both from abstraction of H atoms (alkenes and CO) and from oxygen atom addition followed by decomposition (ketones, aldehydes, and CO_2).

In the presence of molecular oxygen, reaction 3 and subsequent reaction 4 are expected. McDade et al.[12] have reported the rate

(1) Griffiths, J. F. *Adv. Chem. Phys.* **1986**, *64*, 203.
(2) Michael, J. V.; Keil, D. G.; Klemm, R. B. *J. Chem. Phys.* **1985**, *83*, 1630.
(3) Niki, H.; Maker, P. D.; Savage, C. M.; Breitenbach, L. P. *Int. J. Chem. Kinet.* **1985**, *17*, 525.
(4) Slagle, I. R.; Gutman, D. *J. Am. Chem. Soc.* **1982**, *104*, 4741.
(5) Mack, G. P. R.; Thrush, B. A. *J. Chem. Soc., Faraday Trans. 1* **1974**, *70*, 178.
(6) Singleton, D. L.; Irwin, R. S.; Cvetanović, R. J. *Can. J. Chem.* **1977**, *55*, 3321.
(7) Michael, J. V.; Lee, J. H. *Chem. Phys. Lett.* **1977**, *51*, 303.
(8) Washida, N. Abstracts of Papers, International Symposium on Chemical Kinetics Related to Atmospheric Chemistry, Tsukuba, Japan, 1982.
(9) Washida, N.; Bayes, K. D. *J. Phys. Chem.* **1980**, *84*, 1309.
(10) Washida, N. *Bull. Chem. Soc. Jpn.* **1987**, *60*, 3739.
(11) Mack, G. P. R.; Thrush, B. A. *J. Chem. Soc., Faraday Trans. 1* **1973**, *69*, 208.
(12) McDade, C. E.; Lenhardt, T. M.; Bayes, K. D. *J. Photochem.* **1982**, *20*, 1.
(13) Baulch, D. L.; Cox, R. A.; Hampson, R. F., Jr.; Kerr, J. A.; Troe, J.; Watson, R. T. *J. Phys. Chem. Ref. Data* **1984**, *13*, 1259.
(14) Rosenstock, H. M.; Draxl, K.; Steiner, B. W.; Herron, J. T. Energetics of Gaseous Ions. *J. Phys. Chem. Ref. Data, Suppl.* **1977**, *6*(1).

0022-3654/89/2093-5813$01.50/0

TABLE I: Heats of Formation and Ionization Potentials of Molecules

m/e	molecule	$\Delta H_f°(298)$,[a] kcal mol^{-1}	IP,[b] eV	lamp (window)[c]
15	CH_3	34.8	9.84	Kr(MgF_2), Kr(CaF_2)
42	CH_2CO	-14.2	9.61	Kr(MgF_2), Kr(CaF_2)
43	CH_3CO	-5.8	8.05	Xe(sapphire)
44	CH_3CHO	-39.7	10.23	Kr(MgF_2), Ar(LiF)

[a] Quoted from ref 13. [b] Quoted from ref 14. [c] Photon energies: 11.83 and 11.62 eV [Ar(LiF)], 10.64 and 10.03 eV [Kr(MgF_2)], 10.03 eV [Kr(CaF_2)], 8.44 eV [Xe(sapphire)].

constant for reaction 3. But, no direct information on the products of reactions 3 and 4 is available.

$$CH_3CO + O_2 + M \longrightarrow CH_3CO_3 + M \quad (3)$$

$$CH_3CO_3 + O \longrightarrow CH_2CO + OH + O_2 \quad (4a)$$

$$\longrightarrow CH_3 + CO_2 + O_2 \quad (4b)$$

$$\longrightarrow \text{other products} \quad (4c)$$

In the present study, reaction 1 was studied by the discharge-flow method coupled with photoionization mass spectrometry at room temperature (295 ± 4 K). For the conditions of excess atomic oxygen, the rate constant for reaction 1, as well as the branching fractions for 2a and 2b, was measured. In the presence of molecular oxygen, the overall rate constant for reaction 2 relative to reaction 3 was obtained.

By analogy with other hydrocarbon reactions,[9,10] the products of reaction 4 should be $CH_2CO + OH + O_2$ and $CH_3 + CO_2 + O_2$. In the presence of molecular oxygen, we have identified some of the products of reaction 4 and determined the branching fractions for (4a) and (4b).

Experimental Section

The details of the fast-flow reactor and photoionization mass spectrometer (PIMS) have been described previously.[10] A Pyrex flow reactor (12.5-mm i.d.) was used. Oxygen atoms were produced by a microwave discharge of molecular oxygen (diluted in helium) or by a microwave discharge of N_2 followed by the rapid reaction $N + NO \rightarrow O + N_2$. Since no significant difference between these two methods was observed, the O_2 microwave discharge method was usually used. The concentrations of initial oxygen atoms were measured by the titration reaction $O + NO_2 \rightarrow NO + O_2$. NO signals were recorded when NO_2 was added in excess. Acetaldehyde was diluted in helium and was added to the main flow through a movable inlet. Gases were introduced to the photoionization mass spectrometer through a pinhole at the end of the flow tube. Partial pressures of reagent gases, as well as the total pressure, were measured by a capacitance manometer (MKS Baratron 170M-35). The concentrations of reagents and the flow velocity were determined by a separate calibration of the flow rate as a function of pressure, which includes the modification for pressure drop along the flow reactor. All experiments were carried out at room temperature (295 ± 4 K).

Molecules involved in the present study are listed in Table I, together with their heats of formation, ionization potentials, and the light sources (rare-gas resonance lamps powered by microwave discharge) used for ionization.

He (Nippon Sanso; 99.9999%), NO (Matheson; 99.0%), NO_2 (Matheson; 99.5%), N_2 (Nippon Sanso; 99.9995%), O_2 (Nippon Sanso; 99.99%), H_2 (Nippon Sanso; 99.9999%), and acetaldehyde (Merck; 99%) were used without further purification.

Ketene was prepared by the pyrolysis of diketene[15] and purified by trap-to-trap distillation. Ketene was stored at liquid nitrogen temperature in order to avoid dimerization and diluted in helium just prior to use.

All indicated error limits represent 2 standard deviations, and averaged values are weighted averages. All the errors possible to evaluate, such as the uncertainties in the rate constants for the reference reactions used, are included in the evaluation of the error limits for the present results.

(15) Washida, N.; Hatakeyama, S.; Takagi, H.; Kyogoku, T.; Sato, S. *J. Chem. Phys.* **1983**, *78*, 4533.

TABLE II: Summary of $CH_3CHO + O$ Rate Constant (k_1) Measurements

parameter	run no. 1	2	3
O atom source	N + NO	O_2 discharge	O_2 discharge
pressure, torr	3.47	3.41	3.47
temp., K	298	292	292
flow rate, cm s^{-1}	1930	1922	1929
$[O]_0$, molecules cm^{-3}	1.38×10^{14}	3.54×10^{13}	8.00×10^{13}
$[CH_3CHO]_0$, molecules cm^{-3}	6.2×10^{12}	3.1×10^{12}	4.1×10^{12}
k_1, 10^{-13} cm^3 molecule^{-1} s^{-1}	3.77 ± 0.46[a]	3.95 ± 1.16[a]	4.02 ± 0.33[a]

[a] Indicated errors are 2 standard deviations.

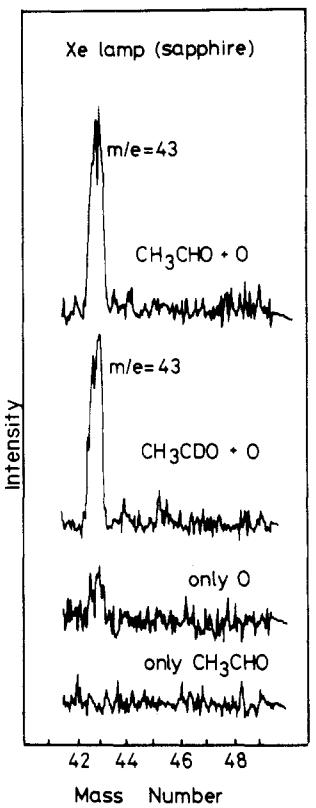

Figure 1. Mass spectra of CH_3CO radical. A Xe lamp with a sapphire window was used for ionization. The neighboring CH_3CHO peak (m/e = 44) was not observed.

Results

A. Rate Constant for Reaction 1. The rate constant for reaction 1 at room temperature was determined from the first-order decay of acetaldehyde signals in an excess of oxygen atoms. Logarithmic signal intensities were plotted against $[\bar{O}]t$, which is a product of the average oxygen atom concentration and the reaction time (stoichiometric factor of 4 was assumed[10]). Initial conditions were kept as $[CH_3CHO]/[O] < 0.1$ so that the competing reaction $CH_3CHO + OH$ would contribute less than 5% to the acetaldehyde decay.

A summary of k_1 measurement is shown in Table II. An averaged value is $k_1 = (3.9 \pm 0.3) \times 10^{-13}$ cm^3 molecule^{-1} s^{-1} (295 ± 4 K). There was no significant difference when the two different sources of atomic oxygen were used.

B. Products Analysis in $O + CH_3CHO$ System. Products in the reaction of acetaldehyde with excess atomic oxygen were analyzed with various ionization light sources. With use of a Xe lamp with a sapphire window, a peak at m/e = 43 was observed (Figure 1). This is attributed to the CH_3CO radical, the expected

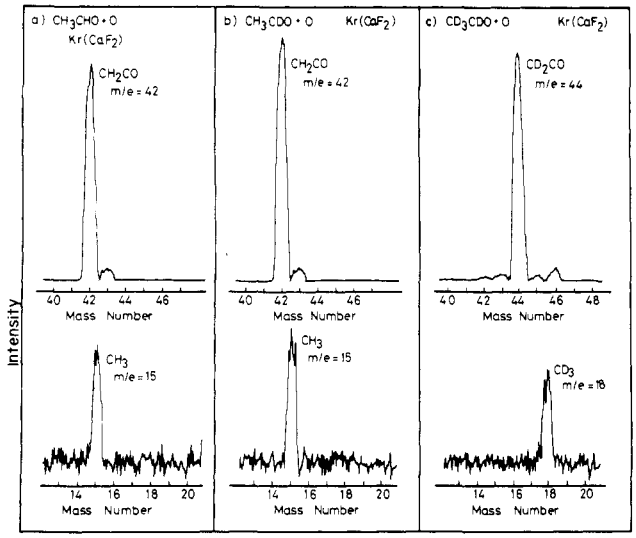

Figure 2. Mass spectra of CH_2CO and the CH_3 radical. A Kr lamp with a CaF_2 window was used.

primary product of reaction 1. Since a peak at the same mass was observed in the reaction of O + CH_3CDO, production of CH_3CO (not CH_2CHO) in reaction 1 was confirmed (>90%). A small signal at m/e = 43 of the trace "only O" in Figure 1 is due to CH_3CHO remaining in the movable inlet when this experiment was done. With use of a Kr lamp with a CaF_2 window, peaks at m/e = 42 and m/e = 15 were observed (Figure 2). Both peaks, ketene (m/e = 42) and methyl radical (m/e = 15), were attributed to the products of the subsequent reaction (2). These products were also confirmed by the use of deuterium-substituted acetaldehydes (CH_3CDO and CD_3CDO). Small peaks at m/e = 43 in Figure 2a,b include contributions from both [^{13}C]ketene and CH_3CO radical. The separation of these can be seen in trace c, where CD_3CO is at m/e = 46 and [^{13}C]ketene is at m/e = 45. No other credible signal was observed.

C. Competition between Reactions of CH_3CO with O and O_2. When O_2 was added to the system, the intensity of the CH_3CO signal decreased. This can be explained by a competition between reactions of CH_3CO with O and O_2 and described by a Stern–Volmer type of equation (5). The superscript 0 refers to the

$$CH_3CO + O \rightarrow \text{products} \quad (2)$$

$$CH_3CO + O_2 + M \rightarrow \text{products} \quad (3)$$

$$\frac{[CH_3CO]^0_{ss}}{[CH_3CO]_{ss}} = 1 + \frac{k_3}{k_2}\frac{[O_2]}{[\bar{O}]} \quad (5)$$

absence of molecular oxygen, the subscript ss refers to the steady-state concentration, and k_2 and k_3 are overall second-order rate constants for reactions 2 and 3, respectively. [$\bar{O}$] is an averaged concentration of oxygen atoms.[10] The slope of a plot of $[CH_3CO]^0_{ss}/[CH_3CO]_{ss}$ vs $[O_2]/[\bar{O}]$ should give the ratio k_3/k_2 (Figure 3). The open circles in Figure 3 are experiments using N + NO as the atomic oxygen source, and the solid circles are experiments with the O_2 microwave discharge. There is no significant difference between the two methods. For the O_2 microwave discharge experiments, small corrections (about 1%) were made for the molecular oxygen that did not decompose in the microwave discharge. In the case of the N + NO experiments, no corrections were made for the CH_3CO + NO reaction (estimated to be about 0.1% using the rate constant for CH_3CO + NO measured by McDade et al.[12]). The resulting ratio k_3/k_2 was (6.3 ± 0.5) × 10^{-3}. With the rate constant for reaction 3 measured previously[12] [k_3 = (2.0 ± 0.4) × 10^{-12} cm^3 molecule^{-1} s^{-1}], k_2 = (3.2 ± 0.7) × 10^{-10} cm^3 molecule^{-1} s^{-1} was obtained.

D. Yields of Ketene and Methyl Radicals. Absolute concentrations of ketene were obtained by separately calibrating the PIMS with known concentrations of ketene. The ketene signal increased with time (Figure 4). The solid circles in Figure 4

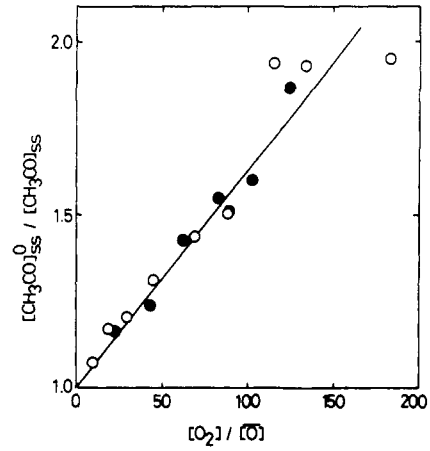

Figure 3. Stern–Volmer plot for the competitive reaction of CH_3CO with O and O_2. Solid circles denote O_2 discharge experiments. Conditions: total pressure, 3.54 Torr; Flow rate, 1938 cm s^{-1}; reaction time, 5.16 ms; $[O]_0$ = 8.81 × 10^{13} molecules cm^{-3}; $[CH_3CHO]_0$ = 3.8 × 10^{12} molecules cm^{-3}. Open circles denote N + NO experiments. Conditions: total pressure, 3.57 Torr; flow rate, 1941 cm s^{-1}; reaction time, 5.15 ms; $[O]_0$ = 3.99 × 10^{13} molecules cm^{-3}; $[CH_3CHO]_0$ = 4.45 × 10^{12} molecules cm^{-3}.

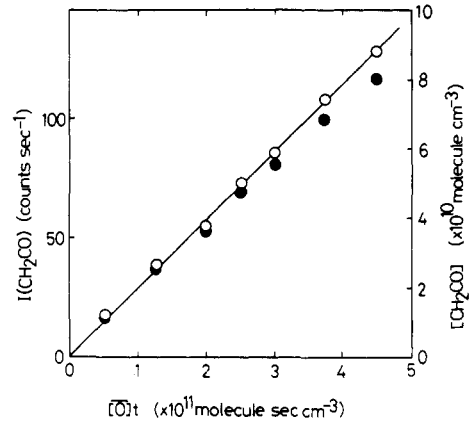

Figure 4. Formation of ketene in the CH_3CHO + O reaction. Conditions: total pressure, 3.28 Torr; flow rate, 1905 cm s^{-1}; $[O]_0$ = 4.83 × 10^{13} molecules cm^{-3}; $[CH_3CHO]_0$ = 2.51 × 10^{12} molecules cm^{-3}. Solid circles and open circles denote $[CH_2CO]_{obs}$ and $[CH_2CO]_{mod}$, respectively (see text).

denote $[CH_2CO]_{obs}$, the observed ketene concentration. The open circles denote $[CH_2CO]_{mod}$, the ketene concentrations that would have been observed if reaction 6 were not consuming ketene.

$$CH_2CO + O \rightarrow \text{products} \quad (6)$$

$[CH_2CO]_{mod}$ is given by eq 7,[15] where k_1 and k_6 are rate constants

$$[CH_2CO]_{mod} = [CH_2CO]_{obs}\frac{(k_1 - k_6)[1 - \exp(-k_1[\bar{O}]t)]}{k_1[\exp(-k_6[\bar{O}]t) - \exp(-k_1[\bar{O}]t)]} \quad (7)$$

for reactions 1 and 6, respectively. A value k_6 = 4.3 × 10^{-13} cm^3 molecule^{-1} s^{-1} [15] was used in the calculation. A linear regression analysis of $[CH_2CO]_{mod}$ vs $[CH_3CHO]_{consumed}$ (=$[CH_3CHO]_0$ [1 − exp(−k_1[$\bar{O}$]t)]) gives the branching ratio for (2a): $f_{2a} = k_{2a}/k_2$. An average of two independent experiments gave f_{2a} = 22 ± 5%. The indicated error limits include the uncertainty in the determination of ketene sensitivity and those in k_1 and k_6.

Determination of the CH_3 sensitivity was accomplished by forming methyl radicals in[16]

$$CH_2CO + H \rightarrow CH_3 + CO \quad (8)$$

The experiments were carried out in an excess of hydrogen atoms,

(16) Michael, J. V.; Nava, D. F.; Payne, W. A.; Stief, L. J. *J. Chem. Phys.* **1979**, *70*, 5222.

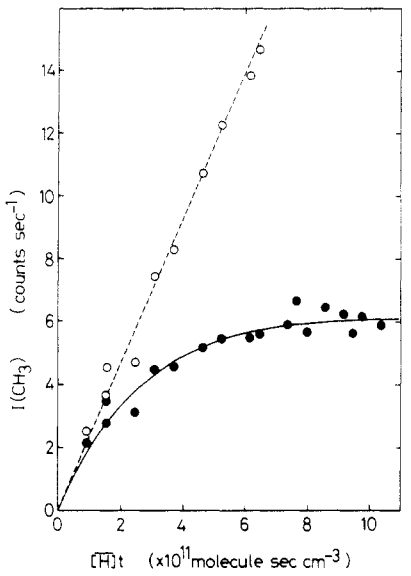

Figure 5. Time dependence of the CH_3 signal in the CH_2CO + H reaction. Conditions: total pressure, 2.50 Torr; flow rate, 1782 cm s^{-1}; $[H]_0 = 5.51 \times 10^{13}$ molecules cm^{-3}; $[CH_2CO]_0 = 1.05 \times 10^{13}$ molecules cm^{-3}. Solid circles and open circles denote $[CH_3]_{obs}$ and $[CH_3]_{mod}$, respectively (see text).

so that one CH_3 is formed for each CH_2CO reacted. The main secondary process should be the reaction

$$CH_3 + H + M \rightarrow CH_4 + M \quad (9)$$

The contribution of the $CH_3 + CH_3$ recombination reaction was small [about $^1/_{20}$th of reaction 9, even if the $CH_3 + CH_3$ recombination rate constant is in the high-pressure limit;[17] second-order rate constant, 6.0×10^{-11} cm^3 $molecule^{-1}$ s^{-1}]. The measured time dependence of $I(CH_3)_{obs}$ (the observed CH_3 signal) is shown in Figure 5 (solid circles). For an excess of hydrogen atoms the concentration of methyl radicals is given by eq 10, where

$$[CH_3] = \frac{k_8[CH_2CO]_0}{k_9 - k_8}[\exp(-k_8[\bar{H}]t) - \exp(-k_9[\bar{H}]t)] \quad (10)$$

k_8 and k_9 are second-order rate constants for reactions 8 and 9, respectively. $[\bar{H}]t$ is a product of the average hydrogen atom concentration and the reaction time. As k_9 is much larger than k_8, the time constant of the exponential increase of CH_3 signal corresponds essentially to $1/(k_9[\bar{H}]t)$. A least-squares fitting to the function $I(CH_3) = A[\exp(-k_8[\bar{H}]t) - \exp(-k_9[\bar{H}]t)]$ gives $k_9 = (3.6 \pm 0.7) \times 10^{-12}$ cm^3 $molecule^{-1}$ s^{-1} (296 K, 2.5 Torr of He). For k_8, a constant 6.2×10^{-14} cm^3 $molecule^{-1}$ s^{-1} [16] was used. Michael et al.[18] have reported a value $k_9 = 5.5 \times 10^{-12}$ cm^3 $molecule^{-1}$ s^{-1} for 2.52 Torr of H_2. So, the present value for k_9 is reasonable considering the difference of third-body efficiencies between H_2 and He. Then, from the value obtained for k_9, $I(CH_3)_{mod}$ was calculated; this is the intensity of the CH_3 signal that would have been observed if no secondary process exists (open circles in Figure 5).

$$I(CH_3)_{mod} = I(CH_3)_{obs}\frac{(k_8 - k_9)[1 - \exp(-k_8[\bar{H}]t)]}{k_8[\exp(-k_9[\bar{H}]t) - \exp(-k_8[\bar{H}]t)]} \quad (11)$$

From the dashed line in Figure 5, $S(CH_3)$ (CH_3 sensitivity) was determined; $S(CH_3) = I(CH_3)_{mod}/[CH_2CO]_{consumed}$. The ratio of sensitivities for CH_3 to NO $[S(CH_3)/S(NO)]$ was 3.5 ± 0.7.

The yield of CH_3 was determined by changing the initial concentration of acetaldehyde and observing the CH_3 signals at fixed reaction time. $I(CH_3)_{obs}$ was converted to absolute concentration ($[CH_3]_{obs}$) by the measured CH_3 detection sensitivity.

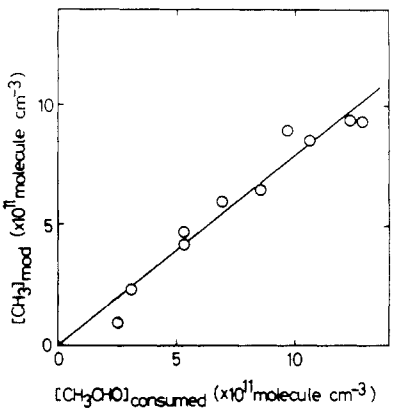

Figure 6. Plot of $[CH_3]_{mod}$ vs $[CH_3CHO]_{consumed}$. Conditions: total pressure, 3.37 Torr; flow rate, 1917 cm s^{-1}; reaction time, 5.22 ms; $[O]_0 = 4.01 \times 10^{13}$ molecules cm^{-3}.

The modified methyl concentration, correcting for consumption by reaction 12, is given by eq 13. A value $k_{12} = 1.38 \times 10^{-10}$

$$CH_3 + O \rightarrow CH_2O + H \quad (12)$$

$$[CH_3]_{mod} = [CH_3]_{obs}\frac{(k_1 - k_{12})[1 - \exp(-k_1[\bar{O}]t)]}{k_1[\exp(-k_{12}[\bar{O}]t) - \exp(-k_1[\bar{O}]t)]} \quad (13)$$

cm^3 $molecule^{-1}$ s^{-1} was used in this calculation. This value was taken from ref 19 and agrees with the recent direct measurement by Slagle et al.[20] The plot of $[CH_3]_{mod}$ vs $[CH_3CHO]_{consumed}$ gives f_{2b} $(=k_{2b}/k_2)$; see Figure 6. An average of two independent experiments gave $f_{2b} = 76 \pm 24\%$. The indicated error includes the uncertainties in $S(CH_3)$, k_1, and k_{12}.

E. Yields of Ketene and Methyl Radicals in the Presence of O_2. In the presence of molecular oxygen and excess atomic oxygen, reaction 3 and the subsequent reaction (4) will occur:

$$CH_3CO + O_2 + M \longrightarrow CH_3CO_3 + M \quad (3)$$

$$CH_3CO_3 + O \longrightarrow CH_2CO + OH + O_2 \quad (4a)$$

$$\longrightarrow CH_3 + CO_2 + O_2 \quad (4b)$$

$$\longrightarrow \text{other products} \quad (4c)$$

When the concentration of O_2 was increased, both the CH_3 signals and the CH_2CO signals decreased. This observation can be explained if the branching fractions for reactions 4a and 4b differ from those for reactions 2a and 2b. The yields of these two products should then be described by[10]

$$\frac{[CH_2CO]_{mod}}{[CH_3CHO]_{consumed}} = f_{2a} + \frac{X}{1 + X}(f_{4a} - f_{2a}) \quad (14)$$

$$\frac{[CH_3]_{mod}}{[CH_3CHO]_{consumed}} = f_{2b} + \frac{X}{1 + X}(f_{4b} - f_{2b}) \quad (15)$$

where

$$X = \frac{k_3[O_2]}{k_2[\bar{O}]} \quad (16)$$

f_{4a} and f_{4b} are the branching fractions for reaction pathways 4a and 4b, $[CH_2CO]_{mod}$ and $[CH_3]_{mod}$ are the modified concentrations of ketene and methyl radicals as given by eq 7 and 13, and $[CH_3CHO]_{consumed} = [CH_3CHO]_0[1 - \exp(-k_1[\bar{O}]t)]$. Thus, f_{4a} and f_{4b} can be determined by plotting $[CH_2CO]_{mod}/[CH_3CHO]_{consumed}$ or $[CH_3]_{mod}/[CH_3CHO]_{consumed}$ vs $X/(1 + X)$. This should give f_{2a} or f_{2b} as intercepts and $f_{4a} - f_{2a}$ or $f_{4b} - f_{2b}$ as slopes. Plots of the data appear linear, as shown in Figure 7, and give $f_{4a} = -8 \pm 10\%$ (<10%) and $f_{4b} = 27 \pm 25\%$. Other

(17) Slagle, I. R.; Gutman, D.; Davice, J. W.; Pilling, M. J. *J. Phys. Chem.* **1988**, *92*, 2455.
(18) Michael, J. V.; Osborne, D. T.; Suess, G. N. *J. Chem. Phys.* **1973**, *58*, 2800.
(19) Washida, N. *J. Chem. Phys.* **1980**, *73*, 1665.
(20) Slagle, I. R.; Sarzyński, D.; Gutman, D. *J. Phys. Chem.* **1987**, *91*, 4375.

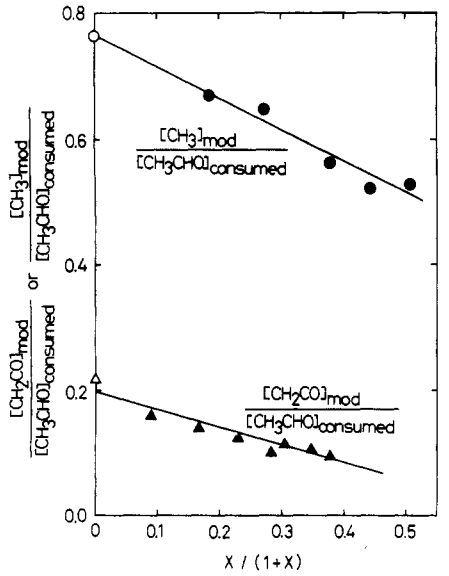

Figure 7. Determination of product fractions for channels 4a and 4b. Triangles and circles denote $[CH_2CO]_{mod}/[CH_3CHO]_{consumed}$ and $[CH_3]_{mod}/[CH_3CHO]_{consumed}$, respectively. An open triangle and an open circle denote data points from separate experiments (see text). Conditions ($[CH_2CO]$ measurement): total pressure, 3.35 Torr; flow rate, 1914 cm s^{-1}; reaction time, 5.22 ms; $[O]_0 = 4.83 \times 10^{13}$ molecules cm^{-3}; $[CH_3CHO]_0 = 2.94 \times 10^{12}$ molecules cm^{-3}. Conditions ($[CH_3]$ measurement): total pressure, 3.59 Torr; flow rate, 1944 cm s^{-1}; reaction time, 5.14 ms; $[O]_0 = 4.57 \times 10^{13}$ molecules cm^{-3}; $[CH_3CHO]_0 = 1.29 \times 10^{13}$ molecules cm^{-3}.

TABLE III: Comparison of k_1 (Rate Constant for $CH_3CHO + O$)

ref	method	k_1 (room temp),[a] 10^{-13} cm^3 $molecule^{-1}$ s^{-1}
this work	discharge-flow–photoionization, mass spectrometry	3.9 ± 0.3
Singleton et al.[6]	Hg sensitization–chemiluminescence–phase shift	4.3 ± 0.3
Michael and Lee[7]	discharge-flow–resonance fluorescence	4.9 ± 1.0
Mack and Thrush[5]	discharge-flow–chemiluminescence and EPR	4.8 ± 1.0

[a] Indicated errors are 2 standard deviations. Some of the error limits were quoted at 1 standard deviation level in the original reports.

product channels must be important, since $f_{4a} + f_{4b}$ is less than unity. The values for f_{2a} and f_{2b} reported in section D are also included as part of the least-squares calculation and are shown in Figure 7 (for $X/(1 + X) = 0$). The intercepts of the straight lines shown in Figure 7 give $f_{2a} = 20\%$ and $f_{2b} = 76\%$. This value for f_{2a} appears to be a little smaller than the value reported earlier (22 ± 5%), though these two values agree with each other within experimental accuracy. For f_{2a}, the value reported in section D is more credible. The negative value for f_{4a} is due to experimental error and is considered to be zero (<10%) within experimental accuracy.

A contribution of reaction 17 was estimated from the rate constant for this reaction obtained by Washida[19] and was less than 5% at the maximum O_2 concentration used.

$$CH_3 + O_2 + M \rightarrow CH_3O_2 + M \qquad (17)$$

Discussion

A comparison of the present k_1 measurement with other recent studies is given in Table III. The current value for k_1 is 10–20% smaller than the other measurements. The reasons for this discrepancy are not clear. It should be noted that all of the other measurements were observations of atomic oxygen consumption,

TABLE IV: Rate Constants for R• + O Reactions

R•	IP, eV	rate const, 10^{-10} cm^3 $molecule^{-1}$ s^{-1}	f_{add}[a]	f_{abs}[b]	ref
tert-butyl	6.93	8.7	0.20	0.80	9, 26
cyclohexyl	7.40	2.7[c]	0.48	0.52	22
isopropyl	7.5	4.9[d]	0.39[e]	0.61[e]	10
acetyl	8.05	3.2	0.76	0.22	this work
ethyl	8.51	2.2	0.72	0.23	23
formyl	8.55	2.1	0.46[f]	0.54[f]	24
methyl	9.84	1.4	1	0	20

[a] Branching fractions for the addition pathway(s). [b] Branching fractions for the abstraction pathway. [c] Wu and Bayes[25] calculated this value from their rate constant for O_2 + cyclohexyl radical, together with relative rate measurement in ref 22. [d] Estimated from the ratio of rate constants for reactions of isopropyl-d_6 $[(CD_3)_2CH]$ radical with O_2 and O[10] and the absolute rate constant for the reaction of $(CH_3)_2CH$ with O_2.[27] [e] Branching fractions for the $(CD_3)_2CH + O$ reaction. [f] From ref 11.

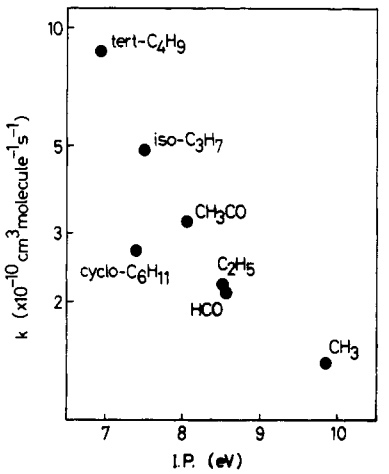

Figure 8. Plot of the rate constant (k) for the R• + O reaction vs the ionization potential (IP) of the radical R•.

and these methods require very low concentrations of atomic oxygen or stoichiometric corrections for the contribution of rapid subsequent reactions. Consequently, the present value for k_1 was used in the above analysis.

Production of acetyl radicals (not vinoxy radicals) in reaction 1 was confirmed with deuterated acetaldehyde (CH_3CDO). In the reaction of nondeuterated acetaldehyde, abstraction of aldehydic hydrogen should be even more dominant, because hydrogen abstractions are usually faster than deuterium abstractions. (For example, experiments on the reaction of oxygen atoms with deuterated propanes show that hydrogen abstraction is strongly favored.[10]) This fact is ascribed to the low aldehydic C–H bond energy (86 kcal mol^{-1}) compared to the methyl group C–H bond energy (≃98 kcal mol^{-1}). Also, in the reaction of CH_3CHO with Cl,[4] abstractions of aldehydic hydrogen are dominant. Kleinermanns and Luntz[21] showed that this abstraction by oxygen atoms proceeds via a direct mechanism.

The rate constant for reaction 2 was determined relative to reaction 3. With the value for k_3 obtained by McDade et al.,[12] k_2 was calculated. While no previous measurements for this reaction have been available, measurements for the other reactions of organic radicals with atomic oxygen have. The rate constants for these reactions are summarized in Table IV, together with the present rate constant for reaction 2. There appears to be a

(21) Kleinermanns, K.; Luntz, A. C. *J. Chem. Phys.* **1982**, *77*, 3774.
(22) Washida, N.; Takagi, H. *J. Am. Chem. Soc.* **1982**, *104*, 168.
(23) Slagle, I. R.; Sarzyński, D.; Gutman, D.; Miller, J. A.; Melius, C. F. *J. Chem. Soc., Faraday Trans. 2* **1988**, *84*, 491.
(24) Washida, N.; Martinez, R. I.; Bayes, K. D. *Z. Naturforsch.* **1974**, *29A*, 251.
(25) Wu, D.; Bayes, K. D. *Int. J. Chem. Kinet.* **1986**, *18*, 547.
(26) Lenhardt, T. M.; McDade, C. E.; Bayes, K. D. *J. Chem. Phys.* **1980**, *72*, 304.

trend of increasing rate constants with decreasing ionization potentials (IP; Figure 8). Such trends were observed in $R^{\bullet} + O_2$ reactions,[27] $R^{\bullet} + O_3$ reactions,[28] and $R^{\bullet} + Cl_2$ reactions[29] and explained by long-range attractive potentials.[28] Despite the structural differences between R•'s (some contain the C=O group, others not), there is a good correlation between log k and IP for the reactions listed in Table IV, except for the cyclohexyl radical + O reaction. Thus, the rate constants for these reactions without (or with small) energy barriers should be largely determined by the long-range forces between the radical and O atom.

The product channels of reaction 2 were well established in the present study. The unimolecular decomposition of acetyl radicals is too slow to contribute at room temperature (3.6 s^{-1} at 298 K, calculated from the temperature-dependent formula of Watkins and Word[30]). Therefore, the observed ketene and methyl radicals are products of reactions 2a and 2b. A sum of the fractions for

$$CH_3CO + O \xrightarrow{0.22} CH_2CO + OH \quad \Delta H = -59 \text{ kcal mol}^{-1} \quad (2a)$$

$$\xrightarrow{0.76} CH_3 + CO_2 \quad \Delta H = -113 \text{ kcal mol}^{-1} \quad (2b)$$

pathways 2a and 2b is equal to unity within experimental error. Branching fractions for the other reactions of organic radicals with atomic oxygen are also summarized in Table IV. At least for noncyclic alkyl radicals, there is a trend of increasing fractions for the abstraction pathway with an increase in the number of hydrogen atoms that can be abstracted. The branching fractions for the reaction of CH_3CO are similar to those for the reaction of C_2H_5, a molecule that contains the same number of (three) abstractable hydrogen atoms as CH_3CO. The formyl radical will be an exception because the C–H bond energy of this radical (17 kcal mol^{-1}) is much smaller than the other radicals ($\simeq$40 kcal mol^{-1}).

When molecular oxygen was added to the system, the yields of both ketene and methyl radicals decreased. Consequently, reaction 4c must be significant. Reactions 4a and 4b will be analogous to reactions 2a and 2b (where the O_2 molecule is thought to be only a chaperon). The decrease of ketene formation when O_2 is added to CH_3CO is reasonable because the exothermicity for the abstraction pathway (4a) is relatively small [$\Delta H \simeq -31$ kcal mol^{-1} for (4a) and $\Delta H \simeq -86$ kcal mol^{-1} for (4b), while they are −59 and −113 kcal mol^{-1} for (2a) and (2b), respectively]. This is the case for the O + $(CH_3)_3CO_2$ reaction[9] and the O + $(CD_3)_2C(H)O_2$ reaction.[10] However, if reaction 4b proceeds via abstraction of the O atom in the C–O–O• group, reaction 4b is not analogous to reaction 2b.

There are unresolved problems in the mechanism and products when molecular oxygen is present. The sum of the fractions for (4a) and (4b) appears to be less than unity.

$CH_3O + CO + O_2$ are conceivable as products of reaction 4. Thus, we tried to detect methoxy radicals using the laser-induced fluorescence (LIF) method, exciting the 2′–0″ band of the A^2A_1–X^2E transition.[31] An increase in the fluorescence signal was observed when the O_2 concentration increased. Thus, the other products of reaction 4 may be $CH_3O + CO + O_2$. However, this LIF experiment was carried out with another reactor (without PIMS), and quantitative information on $[O]_0$, etc., was not available. Further quantitative experiments on CH_3O formation are necessary to get reliable conclusions.

Methoxy radicals will also be formed in the radical–radical reactions 18[32] and 19[33] following reaction 17 or in reaction 20. But, the concentration of CH_3 should be low because reaction 12 is very fast, and the concentration of CH_3O_2 should also be low because reaction 17 is slow and the subsequent reaction of CH_3O_2 with O atoms will be sufficiently fast. Consequently, it is unlikely

$$2CH_3O_2 \rightarrow 2CH_3O + O_2 \quad (18)$$

$$CH_3 + CH_3O_2 \rightarrow 2CH_3O \quad (19)$$

$$CH_3 + CH_3CO_3 \rightarrow CH_3O + CH_3 + CO_2 \quad (20)$$

that these reactions could account for the observed decrease of CH_3 radical in the presence of molecular oxygen, although the observed methoxy radicals may be due to these reactions.

To explain the unresolved problems in the presence of molecular oxygen, it is also conceivable that there are other product channels for reaction 3. Michael et al.[2] have reported a regeneration of OH radicals in the OH + CH_3CHO reaction when O_2 was added. They also reported the formation of OH radicals in the Cl + $CH_3CHO + O_2$ reaction. If OH radicals are formed directly in reaction 3, there may be other product channels for reaction 3 such as $C_2H_2O_2$ (α-lactone) + OH or $CH_2O + CO + OH$. ($CH_3O + CO_2$ is also probable.) But, the formation of CH_3CO_3 in reaction 3 has been well established;[34] (though 100% formation of CH_3CO_3 has not been directly confirmed) it is unlikely that there are significant other product channels for reaction 3. Thus, the most probable explanation for the kinetics in the presence of molecular oxygen is to consider another product channel ($CH_3O + CO + O_2$) for reaction 4.

Acknowledgment. We thank Prof. Kyle D. Bayes (UCLA) for his kind and helpful suggestions and comments regarding this study.

Registry No. H_2, 1333-74-0; O, 17778-80-2; O_2, 7782-44-7; CH_3CHO, 75-07-0; CH_3CO, 3170-69-2.

(27) Ruiz, R. P.; Bayes, K. D. *J. Phys. Chem.* **1984**, *88*, 2592.
(28) Paltenghi, R.; Ogryzlo, E. A.; Bayes, K. D. *J. Phys. Chem.* **1984**, *88*, 2595.
(29) Timonen, R. S.; Russel, J. J.; Sarzyński, D.; Gutman, D. *J. Phys. Chem.* **1987**, *91*, 1873.
(30) Watkins, K. W.; Word, W. W. *Int. J. Chem. Kinet.* **1974**, *6*, 855.
(31) Inoue, G.; Akimoto, H.; Okuda, M. *J. Chem. Phys.* **1980**, *72*, 1769.
(32) Kan, C. S.; Calvert, J. G.; Shaw, J. H. *J. Phys. Chem.* **1980**, *84*, 3411.
(33) Keiffer, M.; Pilling, M. J.; Smith, M. J. C. *J. Phys. Chem.* **1987**, *91*, 6028.
(34) Basco, N.; Parmar, S. S. *Int. J. Chem. Kinet.* **1985**, *17*, 891.